A New Methodology for Determining Thermal Properties and Modelling Temperature Development in Hydrating Concrete

John J. O'Donnell BE, PhD, MIEI
Lecturer, Dept. of Civil/Structural Engineering,
Dublin Institute of Technology.

Eugene J. O'Brien MSc, PhD, CEng, FIEI, MIStructE
Head of Civil Engineering, University College Dublin.

Abstract

A method is described for determining both the rate of heat generation and the time-dependent thermal properties of concrete so that the temperature development in a concrete section can be modelled. The method uses measured temperature data from concrete prisms and involves fitting data from the sample prisms of concrete to a simple theoretical heat-flow model. It is intended to facilitate on-site tests of concrete mixes; the resulting data can be used in computer models to predict the stresses that can lead to early thermal cracking in large pours.

The method is tested by using the thermal properties obtained from the model to predict the temperature versus time profile at a number of locations in a large rectangular block of concrete and comparing these predictions with measured temperatures from the block.

1. INTRODUCTION

It is well known that the setting of concrete involves exothermic chemical reactions (1). When large concrete sections, such as thick walls or deep foundations, are being poured it is often required to control (usually minimise) temperature rise in the concrete. The simplest control measure that can be adopted is to minimise the rate of hydration (and consequently the rate of heat generation) in a given member. This can be done by using the minimum cement content consistent with other design criteria, using a cement with low heat evolution characteristics or replacing some of the cement with a pozzolan such as pulverised fuel ash or blast-furnace slag (5). Minimising the concrete placing temperature and choosing an appropriate formwork type can also be beneficial.

In general, if a large section is being cast the main factor to be controlled is the temperature difference between the core and the surface. If a thin member cast onto existing mature concrete is involved then the maximum overall temperature rise is the critical factor.

In order to decide what control method is appropriate and to estimate the thermal stresses that may arise in the concrete it is of great benefit to be able to estimate the full temperature/time history of the concrete during hydration. A knowledge is needed of both the rate of heat generation and the other thermal properties of the concrete if the complete temperature/time history of the concrete structure is to be modelled numerically.

A number of methods have been described in the literature for determining the relevant properties, with most attention being paid to the rate of heat generation. The use of controlled adiabatic tests has been described by a number of authors in this context (2,3). In one study, measured temperatures from three adiabatic samples were combined to determine the heat generation properties of a concrete mix (3). Large insulated blocks have also been used to approximate adiabatic conditions (4). In another approach isothermal calorimetry on a cement sample was used to estimate the rate of heat generation (5).

In this paper a method is described whereby three short prisms of fresh concrete are used to estimate the required thermal properties. While the prisms are stored in different ambient conditions, none have to be stored in a carefully controlled thermal environment. This flexibility in the thermal environment renders the method particularly suitable for use on site.

In each prism, temperature is monitored at a number of nodes along the axis. A one-dimensional theoretical model is then formulated where the unknown properties consist of the thermal properties and the quantities relating to heat generation. A standard optimisation algorithm is used to find the property values that give the closest match of theoretical to actual temperature profiles.

To test the accuracy of this approach, the property values obtained were used in a finite element model of a large rectangular block of concrete. The temperature profiles predicted by this model were compared with temperatures measured in the block. This provided a measure of the accuracy of the thermal property values obtained from the optimisation.

2. EXPERIMENTAL PROGRAMME

A total of five concrete specimens were cast in the test. They comprised three short prisms, one long prism and one partially insulated block. The aim was to use measured temperatures from the prisms to predict temperatures in the block and to compare these predictions with measured values. The long prism was used to determine the heat loss coefficients for the sides and ends of the prisms.

All specimens were cast indoors using Ordinary Portland Cement. The constituents of the mix are given in Table 1.

Fine aggregate (sand)	545 kg.
Coarse aggregate (10mm)	1010 kg.
Ordinary Portland Cement	595 kg.
Water	230 kg.

Table 1 - Concrete mix constituents, per m^3 of concrete

The fine aggregate, coarse aggregate and cement were initially mixed manually as a single batch until a uniform matrix was obtained. Due to the limited size of the mixer used the addition of the water and the final mixing was done in two batches, one batch being used for the prisms and the second being used for the block. There was a time delay of approximately twenty minutes between the mixing of the two batches. This time delay was recorded and was allowed for when the results were being analysed.

The short prisms used are illustrated in Figures 1 and 4. All the prisms contained 5mm thick steel plates at the locations shown. Each concrete prism was 450mm long (including the steel plates) with a 100mm x 100mm cross section. These plates were placed for purposes outside the scope of this paper. Prism Nos. 1 and 3 were stored at a room temperature of about 15 ^{o}C. Prism No. 2 was initially stored at room temperature and after eight hours was placed in an oven, at about 50 ^{o}C. It was then alternated every eight hours, between the oven environment and the room temperature environment. This was done so that a temperature difference was always maintained between the concrete in the prism and its environment.

Each prism contained a 20 mm diameter hollow plastic tube along its axis. Thermocouples were placed along the tube at the locations shown in Fig. 1. The thermocouple wires were passed through the plastic tube to the outside of each prism. Temperatures were recorded, at fifteen minute intervals, for a period of seven days, the first set of readings being taken approximately fifteen minutes after the second batch of concrete was mixed. Additional thermocouples were used to record room and oven ambient temperatures.

The long prism is illustrated in Fig. 2. This prism was 950mm long, including ten 5mm thick metal plates, with a 100 mm x 100 mm cross-section. As for the short prisms it contained a 20mm diameter plastic tube along its axis. A total of eight thermocouples were placed on the tube at the locations indicated in the figure. The prism was lined on all sides, except one end face, with 50 mm of dense extruded polystyrene.

The long prism was initially stored in an oven at about 40 ^{o}C for a period of two weeks to ensure that the hydration rate had reduced to a negligible level, that is, the concrete had matured. At the end of the two week period the prism was initially heated up to a temperature of approximately 50 ^{o}C and was then removed from the oven to a room temperature environment of about 15 ^{O}C. Temperatures were monitored along its axis, at five minute intervals, until it had cooled to within about 5 ^{o}C of ambient temperature. The prism was then put back into the oven (at about 50 ^{o}C) and thermocouple readings were again taken at five minute intervals until the prism concrete had heated up to within 5 ^{o}C of oven temperature. This cooling/heating procedure was repeated a number of times with temperatures being recorded for each cycle. Additional thermocouples were used to record room and oven ambient temperatures throughout the test.

The block dimensions were 300mm x 500mm x 1000mm as illustrated in Figures 3 and 5. All faces were lined with 50mm of polystyrene except for one 300mm x 500mm face and one 300mm x 1000mm face which were lined with plywood only. This arrangement was chosen to simulate a horizontal “slice” through a thick concrete wall or abutment. Six thermocouples were placed in the block. The gauges were placed in the plane midway between the two 500mm x 1000mm insulated faces at the locations indicated in the figure. Readings were recorded at 15 minute intervals for a period of seven days.

Type K thermocouples were used throughout. Each thermocouple was microwelded at its end and connected to a data-logger. The data-logger was attached to a personal computer which recorded and stored all of the temperature readings.

3. THEORETICAL DEVELOPMENT

3.1 Heat flow equations for the short prisms

Heat flow in the prisms is largely uni-axial and can be approximated with a one-dimensional model, modified to allow for out-of-axis heat losses. It follows that the temperature (T) at any point along each prism axis is a function of two independent variables, namely, distance along the prism axis (x) and time (t);

$$T = T(x,t) \tag{1}$$

Applying standard heat transfer theory, a number of equations can be developed. The temperature distribution in the interior of the prisms is governed by Equation (2) while Boundary Equations (3) and (4) define the temperature gradient at the insulated and uninsulated ends of the prism respectively:

$$\frac{\partial T}{\partial t} = R_0\left[k_0\left(\frac{\partial^2 T}{\partial x^2}\right) + g_0 - L'_p\,(T - T_a)\right] \tag{2}$$

$$\left(\frac{\partial T}{\partial x}\right)_{x=0} = \frac{h'_1}{k_0}(T_1 - T_a) \tag{3}$$

$$\left(\frac{\partial T}{\partial x}\right)_{x=L} = \frac{h'_2}{k_0}(T_L - T_a) \tag{4}$$

where $R_0 = \dfrac{\rho_m c_m}{\rho c}$,

with ρ = density of the concrete (kg/m^3) at time t,

ρ_m = density of mature concrete (kg/m^3),

c = specific heat capacity of the concrete at time t (J/kg.^{o}C),

c_m = specific heat capacity of mature concrete (J/kg.^{o}C),

and $k_0 = \dfrac{k}{\rho_m c_m}, g_o = \dfrac{g}{\rho_m c_m}, h'_1 = \dfrac{h_1}{\rho_m c_m}, h'_2 = \dfrac{h_2}{\rho_m c_m}, L'_p = \dfrac{L_p}{\rho_m c_m}$

with k = conductivity of the concrete (W/m.^{o}C),

$g = g(x,t)$ = rate of internal heat generation (W/m^3),

h_1 = combined heat transfer coefficient at the uninsulated end, which includes for convection and radiation from the plywood surface as well as conduction through the plywood (W/m^2. ^{o}C),

h_2 = combined heat transfer coefficient at the insulated end, which includes for

convection and radiation from the plywood surface as well as conduction through the insulation and plywood (W/m^2. ^{o}C),

T_1 = temperature on the prism axis just inside the plywood at the uninsulated end (^{o}C),

T_a = ambient temperature (^{o}C),

T_L = temperature on prism axis just inside the insulation at the insulated end (^{o}C) ,

L_p = heat loss coefficient for the out-of -axis heat losses (W/m^3. ^{o}C) .

The normalised total heat generated per unit volume (often called the maturity) at a distance x along the prism axis up to time t can be expressed as:

$$Q(x,t) = \int_{t_0}^{t} g_o(x,t)dt \tag{5}$$

where Q = normalised total heat generated (^{o}C), at time t.

The rate of heat generation can be modelled by the Arrhenius equation (6) to give:

$$g_0 = g_r \exp - K\left(\frac{1}{(T+273)} - \frac{1}{(T_r+273)}\right) \tag{6}$$

where T_r = an arbitrary reference temperature (^{o}C),

g_r = the value of the heat generation parameter at the reference temperature,

and $K = \frac{E}{R}$ is a constant (^{o}K)

with E = activation energy for the hydration reaction (kJ/mole),

R = Gas Constant (kJ/mole.^{o}K).

273 is added to each ^{o}C temperature to convert it to ^{o}K because the Arrhenius equation uses absolute temperatures in degrees Kelvin.

Substituting Equation (6) in Equation (2) gives:

$$\frac{\partial T}{\partial t} = R_0\left[k_0\left(\frac{\partial^2 T}{\partial x^2}\right) + g_r \exp - K\left(\frac{1}{(T+273)} - \frac{1}{(T_r+273)}\right) - L'_p\,(T - T_a)\right] \tag{7}$$

Equations (3), (4) and (7) determine the temperature distribution in the prisms throughout the hydration period. A total of seven unknown parameters can be identified in these equations, namely g_r, k_0, R_0,K, h'_1 ,h'_2 , L'_p . The first two parameters - g_r and k_0, - representing heat generation and conductivity respectively, are assumed to be unique

functions of maturity (Q). The assumption regarding g_r is supported by existing literature (10,11). With regard to k_0, the conductivity of concrete does not vary significantly with temperature in the normal ambient range (1) and, accordingly, it was not considered necessary to allow this parameter to vary as a function of temperature. Conductivity will change somewhat as the amount of free water in the concrete changes and this in turn depends on the degree of hydration. Therefore, it is assumed that k_0 varies as a function of Q. Both g_r and k_0, were determined from the temperature data recorded in the short prisms.

The third parameter $R_0 = \frac{\rho_m c_m}{\rho c}$, can usually be assumed to equal unity as neither the specific heat capacity nor the density of the concrete vary significantly throughout the main hydration period.

The remaining four parameters - K, h'_1, h'_2 and L'_p - are assumed to be constants. This assumption is again supported by the literature (11). The first of these parameters - K- was determined from the short prisms while the remaining three were determined from the long prism experiment.

Thus the three parameters representing the heat generation rate and the other thermal properties of concrete, namely, k_0, g_r, K, were determined from the short prism data while the three parameters governing the heat loss rate from the sides and ends of the prism, namely L'_p, h'_1 and h'_2, were determined from the long prism data. A computer program was written to find the values for each set of three parameters that give a best fit of measured temperatures to those predicted by theoretical models of the long and short prisms. The program also calculates Q at each node along the prism at the end of each time step. The program solves the heat flow equations, given above, using the finite difference method and uses a standard, least squares, optimisation procedure to find the best-fit values for the unknown parameters.

3.2 Heat Flow Equations for the Long Prism

As the concrete is mature in the long prism when the temperature measurements are being taken, hydration will have dropped to negligible levels. Therefore, the heat generation term can be set to zero and the R term will equal unity. The temperature/ time gradient for any point along the axis of the prism can be expressed as:

$$\frac{\partial T}{\partial t} = \left[k_{0(m)} \frac{\partial^2 T}{\partial x^2} - L'_p (T - T_a) \right] \qquad (11)$$

where $k_{0(m)}$ = value of the conductivity parameter k_0 for mature concrete

Since the long prism cross section is the same as that used for the short prism, the loss factor L'_p will also be the same. The boundary equations are the same as those already given in Equations (2) and (3) for the short prism.

The loss term, L'_p, was found as follows. Consider the plane of cross-section A-A through the long prism located halfway along the prism axis (Fig. 2). When there is a temperature difference between the prism concrete and the surrounding air, heat flow will occur in this plane. The results of a number of numerical tests, using the finite difference program, showed that, for a prism of this length, the heat flow along the axis of the prism at the location A-A is insignificant compared with the out-of-axis heat flow in the plane of the cross-section. Therefore, the temperature time gradient at the centre of cross-section A-A can be expressed as:

$$\frac{\partial T_c}{\partial t} = L'_p (T_c - T_a) \tag{12}$$

where T_c = temperature at the intersection of the prism axis and section A-A

L'_p = loss factor for prism cross-section

In the laboratory the ambient temperature is relatively constant in comparison with the prism temperature which is changing quite rapidly. Therefore Equation (12) can be rewritten as:

$$\frac{\partial T_c}{\partial t} \approx \frac{\partial T_d}{\partial t} = L'_p (T_d) \tag{13}$$

where $T_d = (T_c - T_a)$ is the difference in temperature between the prism axis, at location A-A, and ambient temperature.

The solution to this differential equation is

$$T_d = \exp(L'_p t) + C \tag{14}$$

where C = an unknown constant.

Taking the natural log of both sides we get

$$\ln T_d = \ln C + L'_p t = (C' + L'_p t) \tag{15}$$

where C' = ln$C$ = a constant

If the long prism is heated up in an oven and is then allowed to cool in a room temperature environment then Equation (15) can be applied to the cooling phase. By plotting $\ln T_d$ against t over a period of time and fitting a straight line to the data, an estimate of L'_p is obtained. Similarly Equation (15) can be applied when the prism is being heated up from ambient to oven temperature with L'_p, in this case, being a heat gain factor.

3.3 Variation of Thermal Properties during Hydration

Two of the unknown parameters determined from the short prism analysis, g_r and k_0, are assumed to be functions of Q. In order to model these parameters using the computer program described at the end of Section 3.1, some assumptions had to be made about how these parameters vary over the range of Q. Two different methods were initially considered; a Global and a Local method. In both approaches the two parameters were assumed to be either constants throughout the time interval or specified functions of Q. A combination of the Local and Global methods was finally adopted when determining the best-fit values for the unknown parameters.

In the Local analysis method the Q range is divided up into a number of 'maturity' bands. Within each band the heat generation term - g_r - is assumed to vary linearly with Q. Thus:

$$g_r(Q) = g_1 + g_2 Q \qquad \text{for each band} \tag{16}$$

where g_1, g_2 are constants

The k_0, term is assumed to be constant within each band. Thus, for each maturity band, the short prism analysis was reduced to finding values for four constant parameters - g_1, g_2, k_0, and K, The values of these four parameters are allowed to vary from one maturity band to the next so that the properties have freedom to vary across the Q range. An optimisation is done for each band to find the values of the parameters that give a best fit of measured temperatures to those calculated by the theoretical model.

The Local Method of analysis has a number of complications. Firstly, for a given prism at any given time, the nodes along the prism axis will be hydrating at different rates and will therefore have different values of Q at any particular time. This can be illustrated by means of an example. Fig. 6 shows a typical case of a prism where temperatures are being monitored at four nodes along the prism axis.

Temperature readings are taken at each node at times t_0, t_1, t_2 and t_3. $Q(i,t_j)$ and $T(i,t_j)$ represent the values of Q and T at node i, at time t_j. In the figure the value of Q is plotted on the vertical axis for each node at the end of each time step (it should be noted that in a real example the Q values at the end of each time step will not be known in advance). The Q range is divided into three maturity bands in this case. These bands are indicated, in the diagram, by the dotted lines.

The figure illustrates how, at any given time (t), the different nodes will have different values of Q. For example, at time t_1 the Q value for node 1 lies in Band 2 while the Q values for nodes 2, 3 and 4 lie in Band 1. It is clear, therefore, that before optimising to find the unknown parameters for any band the temperature readings whose Q values fall into that band must be identified. In the example illustrated in Fig. 6 only four temperature readings have Q values that fall into Band 1, namely, $T(2,t_1)$, $T(3,t_1)$, $T(4,t_1)$ and $T(4,t_2)$. Therefore only these four readings should be used in the optimisation for Band 1.

An iterative method has been developed to identify the temperature readings relevant to each Q band. The method is started by analysing all of the temperature readings (sixteen in the example illustrated in Fig. 5) to get an initial estimate of parameter values for Band 1. These parameter values are then used to calculate Q values corresponding to each temperature reading and any readings with Q values outside Band 1 are eliminated. A second run is carried out with the remaining set of temperature readings to get an improved estimate of the parameter values for Band 1 and these are again used to calculate Q values for each reading. Again any readings with Q values outside Band 1 are eliminated and the optimisation is repeated with the new data set. This procedure is repeated in an iterative manner until the temperature readings relevant to Band 1 have been identified and the corresponding best-fit parameter values have been obtained.. A similar analysis is then carried out for Band 2, Band 3 etc.

It is clear that this iterative procedure requires a large number of optimisations to identify the temperature readings relevant to each band. This makes the Local optimisation method computationally slow. The second difficulty that arises with the Local Method is that discontinuities tend to occur between adjacent bands for the optimised values obtained for the various parameters. This occurs because each band is treated as a separate optimisation problem without regard to continuity with adjacent bands.

Because of the complications arising from the Local Method an alternative approach was examined. This second method was designated “the Global Method”. In the simplest version of the Global Method a single equation is used to represent each unknown property for the entire range of Q. Therefore all of the temperature data is analysed in a single run. This method eliminates both the banding and discontinuity problems discussed in the previous section. It is also much faster, computationally, than the Local Method. However, the major difficulty with the method is finding a single equation that accurately reflects the variation of each property as a function of Q. In general, for the Global Method, the parameters K, h'_1 and h'_2 are assumed to be constants, k_0 is assumed to vary linearly with Q and g_r is assumed to be given by an exponential type function of Q. In practice, it was found that g_r cannot be accurately represented by a single equation. Typically two or more equations are required, each applying to a different part of the Q range, to give a good match to measured data. However this does not alter the principle that one set of equations is used for each parameter to describe its variation over the full range of Q.

After a trial and error process involving the comparison of Local and Global results obtained from the short prism data it was found that the g_0 parameter could be represented adequately by the following functions:

$$g_r(Q) = \left(g_1(Q+g_3)^2\right)\exp\left[-g_2(Q+g_3)^3\right] \quad \text{for } Q < 30 \tag{17}$$

$$= C_1(-C_2Q^{1.5}) \quad \text{for } Q > 30 \tag{18}$$

where g_1, g_2, g_3, C_1 and C_2 are constants

The constants C_1 and C_2 were chosen to ensure continuity of both the function value and its first derivative about the point $Q = 30$. Thus C_1 and C_2 were determined by the values of g_1, g_2 and g_3 and were not additional variables. The short prism analysis, therefore, involved finding the values for five constant parameters - g_1, g_2, g_3, K and k_0 - that give a best fit of measured temperature in the three short prisms to those predicted by a theoretical model.

3.4 Heat Flow Equations for the Large Block

The temperature at an internal point in the mid-plane of the block (midway between the two 500mm X 1000mm faces) is given by the two-dimensional version of Equation (2) with R_0 again being taken to equal unity. As for the prism, the out-of-plane losses at any point are proportional to $(T - T_a)$ where T, in this case, is the temperature at the relevant point on the mid-plane. Therefore, the temperature-time gradient, at an internal point on the mid-plane of the block, is given by:

$$\frac{\partial T}{\partial t} = \left[k_0 \left(\frac{\partial^2 T}{\partial x^2} + \frac{\partial^2 T}{\partial y^2}\right) + g_0 - L_b(T - T_a) \right] \tag{19}$$

where L_b = heat loss factor to allow for losses perpendicular to the mid-plane of the block

The boundary equations for the four side-wall boundaries are all of the form

$$\left(\frac{\partial T}{\partial s}\right)_S = \frac{h'}{k_0}(T_S - T_a) \tag{20}$$

where h' = combined convection and radiation coefficient for the boundary.

T_s = temperature of the concrete just inside the insulation or plywood

$\left(\frac{\partial T}{\partial s}\right)_S$ = temperature gradient at the surface where the s direction is normal to surface

The other terms are as previously defined.

3.5 Finite Element Model for the Large Block

The heat-flow in the large block was modelled using a two-dimensional finite element heat-flow model representing
the mid-plane of the block (see Fig. 3 - Sectional Plan). A heat loss factor was included to account for out-of-plane heat losses. In reality, as the block is 3-dimensional, the method adopted introduces a level of approximation and there may be some 3-D effects that are not allowed for in the model used. An eight-node rectangular element was chosen for the model.

The rectangular block was modelled with an 8 x 4 grid of these elements with each element being 0.125 metres square. The time-step used in the analysis was 150 seconds.

Additional computer code was developed by the first author to allow for a time-varying rate of heat generation, (specifically a rate of heat generation that varied as a function of the total heat generated to date) as well as convection and radiation heat loss from the surface of the block

4. RESULTS

4.1 Long Prism Analysis

The first part of the long prism analysis involved estimating the heat loss factor, L'_p, which governs the out-of-axis heat loss/heat gain. The out-of-axis heat flow at the midpoint along the prism axis is governed by Equation (15). The long prism was initially placed in an oven, at a temperature of approximately 50 ^oC, for a period of two weeks. It was then removed from the oven and temperatures were recorded along its axis as it cooled from 50 ^oC towards an ambient room temperature of about 20 ^oC. Fig. 7 illustrates a plot of $\ln(T_d)$ versus t for this data. The temperature difference, T_d was obtained by subtracting the ambient temperature recorded outside the prism from the temperatures recorded by the temperature gauge located at the centre point of the prism axis (Gauge No. 5). It can be seen that the plot of $\ln(T_d)$ versus t is virtually linear.

The second part of the long prism test involved monitoring temperatures in the prism as it was being heated up from a temperature of about 25 ^oC towards an oven temperature of 50 ^oC. When $ln(T_d)$ is plotted against t for this case a similar plot to that in Fig. 7 is obtained. The whole heating and cooling procedure was then repeated a number of times resulting in a number of plots similar to those in Fig 7. For each such plot, linear regression was used to find the best-fit straight line through the data points and the slope of each such line was calculated. It is clear from equation (15) that the slope of these lines is a measure of L'_p.

From a comparison of the slopes the heat loss factor and the heat gain factor were found to be approximately equal. Accordingly, the average of all the slopes was obtained and this figure was adopted as an estimate for the heat loss/heat gain factor $L_p^{'}$. The following value was obtained from this analysis:

$$L^{'}_{p} = 1.09 \times 10^{-5} \text{ sec}^{-1}.$$

This value was adopted in subsequent analyses for both the long and the short prisms.

The second part of the long prism test involved an analysis of heat flow along the prism axis. The temperature/time gradient at any point along the axis of the long prism is given by Equation (11). The boundary equation for the two ends are given by Equations (3) and (4). Equations (3), (4) and (11) together contain three unknown parameters, namely, $k_{o(m)}$, h'_1 and h'_2. The optimisation procedure was used to find the values of these three parameters that gave a best-fit of measured temperatures, along the long prism axis, to those predicted by a theoretical model. The optimised parameter values obtained from this analysis were as follows:

$$k_{o(m)} = 8.27 \times 10^{-7} \text{ m}^2/\text{sec}$$
$$h'_1 = 1.40 \times 10^{-6} \text{ m/sec}$$
$$h'_2 = 1.68 \times 10^{-7} \text{ m/sec}$$

A typical temperature versus time profile obtained from these parameter values is illustrated in Fig. 8 for Node 1 in the long prism when the prism is losing heat. Figs. 9(a) and 9(b) illustrate actual and best-fit theoretical temperature profiles along the prism axis for one particular time for both the "losing heat" and "gaining heat" phases. It can be seen that a reasonably good match has been obtained between actual and best-fit theoretical temperatures.

4.2 Short Prism Analysis

The measured temperature data from the short prisms was analysed to find the unknown parameters relating to heat generation and conductivity. The temperature/time gradient, along the axes of the short prisms, is given by Equation (2). The boundary conditions at the insulated and uninsulated ends of the prisms are defined by Equations (3) and (4). These three equations contain six unknown parameters - k_0, g_r, K, L'_p, h'_1 , and h'_2. The

three latter parameters were determined from the long prism analysis as described in Section 4.1. Thus, only three parameters - k_0, g_r and K - remained to be determined from the short prism data. These are the parameters which define the concrete conductivity, the rate of heat generation and the temperature dependence of the rate of heat generation respectively.

The long prism analysis determined the parameter $k_{0(m)}$ which represents the conductivity of mature concrete. The general conductivity parameter, k_0, was assumed to vary linearly as a function of Q, reaching a value of $k_{0(m)}$ at $Q = Q_{max}$ where Q_{max} is the maximum Q value obtained at the end of the period during which temperature data was recorded. Thus the conductivity parameter was assumed to be given by:

$$k_0(Q) = k_{0(m)} + k_1(Q_{max} - Q) \tag{19}$$

where k_1 = an unknown constant

The heat generation parameter g_r was assumed to be given by Equations (17) and (18). Thus the short prism analysis was reduced to finding the values of five constant parameters - g_1, g_2, g_3, K and k_1. The best fit results were as follows:

$$g_1 = 4.38 \times 10^{-6}$$

$$g_2 = 6.26 \times 10^{-5}$$

$$g_3 = 11.56$$

$$K = 6019\ (^{o}K)$$

$$k_1 = 1.94 \times 10^{-8}$$

Actual and best-fit theoretical temperature versus time profiles resulting from these best-fit values, for one representative node in each prism, are illustrated in Fig. 10. There is quite good agreement between measured and predicted profiles indicating that the theoretical model has modelled, reasonably accurately, the generation and flow of heat in the short prism samples. Accordingly, the best-fit values given above were used to make the temperature predictions in the block.

4.3 Temperature Predictions for Block

The block is illustrated in Fig. 3. A finite element analysis of this block was carried out using the best-fit thermal property parameters given in Sections 4.1 and 4.2. The optimised h_1' and h_2' parameters were used as heat loss coefficients for the insulated and uninsulated sides of the block respectively. It should be noted that the heat loss

coefficients h_1' and h_2' are not strictly applicable to the boundaries of the block. These loss coefficients were obtained for the ends of the prisms and could include some corner or end effects which are specific to the prism and therefore not strictly applicable to the block. Also there may be corner effects in the block which are not allowed for in the finite element model. However, it was felt that these coefficients were sufficiently accurate for the purposes of the model. Fig. 11 illustrates measured and predicted temperature versus time profiles for Gauge Nos. 1, 2, 3, 5 and 6 in the block. Node 4 has been omitted as its plot is very similar to Node 1.

In general, there is reasonable agreement between measured temperatures and those predicted by the theoretical model. While the shapes of the actual and theoretical temperature profiles are somewhat different, in general the discrepancies are relatively small. All of the graphs show a noticeable deviation between predicted and measured temperatures between approximately fifteen hours and twenty-five hours after the pour with the theoretical profiles showing a sharper peak than the measured profiles. However, the predicted and measured peak temperatures are within 2.5 ^{o}C of each other at all of the nodes. Only one thermocouple showed a persistent deviation between predicted and measured temperatures. This occurred at node 3, which gave a predicted temperature consistently lower than the measured temperature after the peak had been reached. This could possibly be explained by the fact that the optimised heat loss coefficients h_1' and h_2' do not adequately model the corner of the block.

On site, for most practical situations, the temperature profile at the centre and near the surface of a section will be the most critical. The results of the above test give reasonably good agreement between predicted and measured temperature for the centre (node 5) and the midside surface (node 6) of the block.

5. CONCLUDING COMMENTS

A method for determining the thermal properties of concrete is described. It is shown that the method produces properties that can be used to predict, with reasonably good accuracy, the temperature/time profile at various locations in a large concrete member. It is also illustrated how the method can be used to predict the degree of hydration at any point in a concrete specimen.

Various methods have been described in the literature for determining both the rate of heat generation and the temperature rise in concrete due to hydration (2, 3, 4, 5). However, the method described in this paper (hereafter called the prism method) does have some new features that make it particularly suitable for use on site:

(i) The prism samples do not have to be stored in a strictly controlled thermal environment.
(ii) Continuous predicted temperature/time profiles can be obtained from the finite element model. Most currently used temperature prediction methods only predict peak temperature and/or the maximum temperature difference within the structure.
(iii) The finite element model can be used to assess the affect on temperature of various activities on site. For example, if the contractor wants to remove his shuttering from a particular member after, say, two days the finite

element model could be used to assess the effect that this would have on the maximum temperature difference occuring in that member.

(iv) The prism method of calculating the total heat generated (Q), is based on temperature measurements from prisms made with the same concrete as that used in the main structure. In contrast, the maturity and degree of hydration methods of strength prediction currently in use involve general functions which can be applied to any given mix. Thus the prism method should be more reliable if a non-standard mix was used.

(v) The prism method can also predict the total heat generated (Q) in the concrete at any given location and time and this can be used to predict the strength of the concrete. Therefore, temperature and strength predictions can be obtained using a single method whereas, at present, separate methods are required.

The prism method has a number of potential practical applications. Firstly it could be used on site throughout the construction phase of a project to make temperature and strength predictions for the various concrete pours. Ideally a set of prisms would be cast each time there is a (large) concrete pour. In this way, a database of information would be built up, which would provide information for ongoing temperature and strength predictions that would be useful in controlling operations on site. For example, the temperature and strength predictions could be used to decide the timing of operations such as formwork removal and the application of post-tensioning forces.

Secondly the prism method could be used as part of a trial mix process. For example, if a certain concrete mix was being proposed for a large concrete structure there might be concerns that large temperature rises could occur, which could lead to lead to early thermal cracking. In this situation it would be possible to do a trial mix, cast and monitor some prisms and, using the measured temperatures from the prisms, make temperature predictions for the main structure. If the predicted temperatures were too high the concrete mix could be adjusted or some other method specified to limit temperature rise.

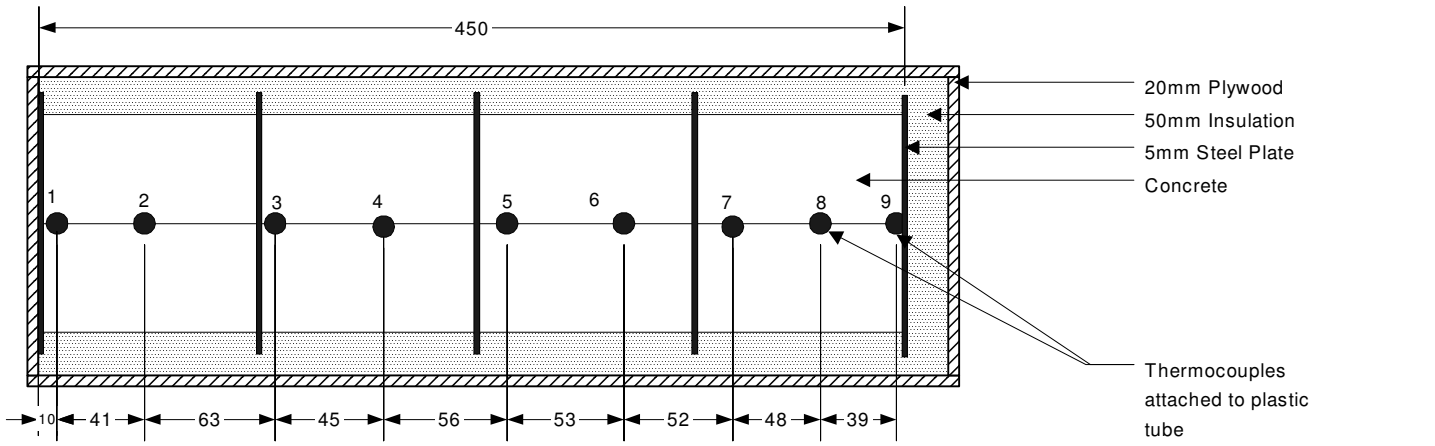

Prism Number 1

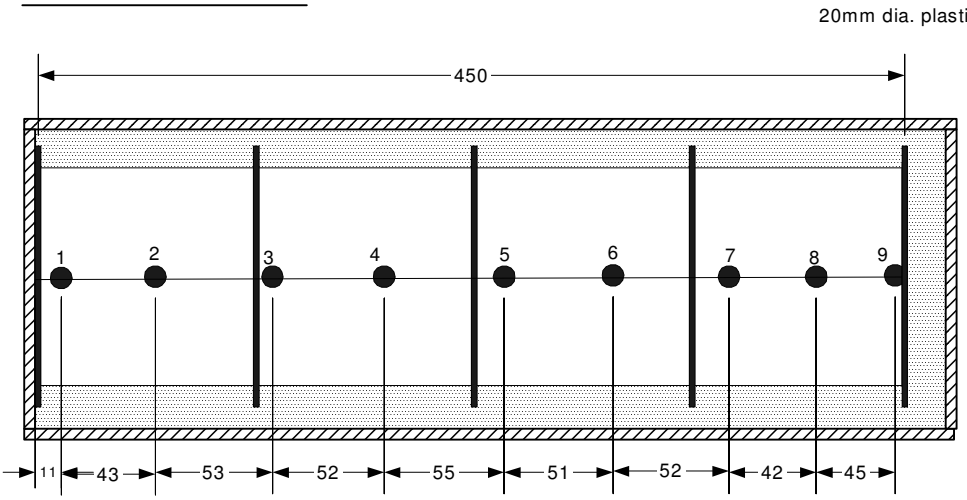

Prism Number 2

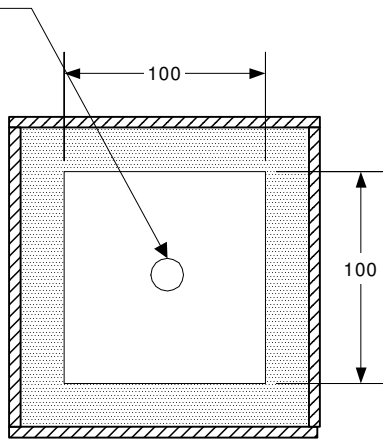

Cross-section

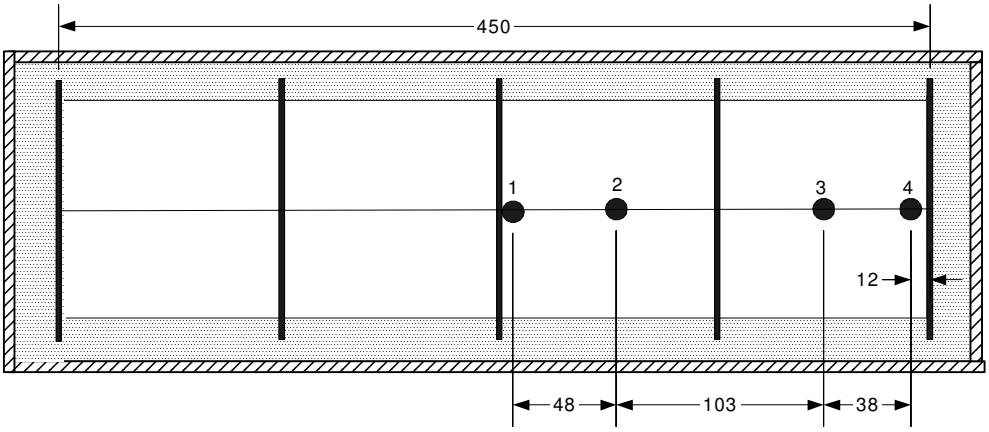

Prism Number 3

Fig. 1 Short Prism Details

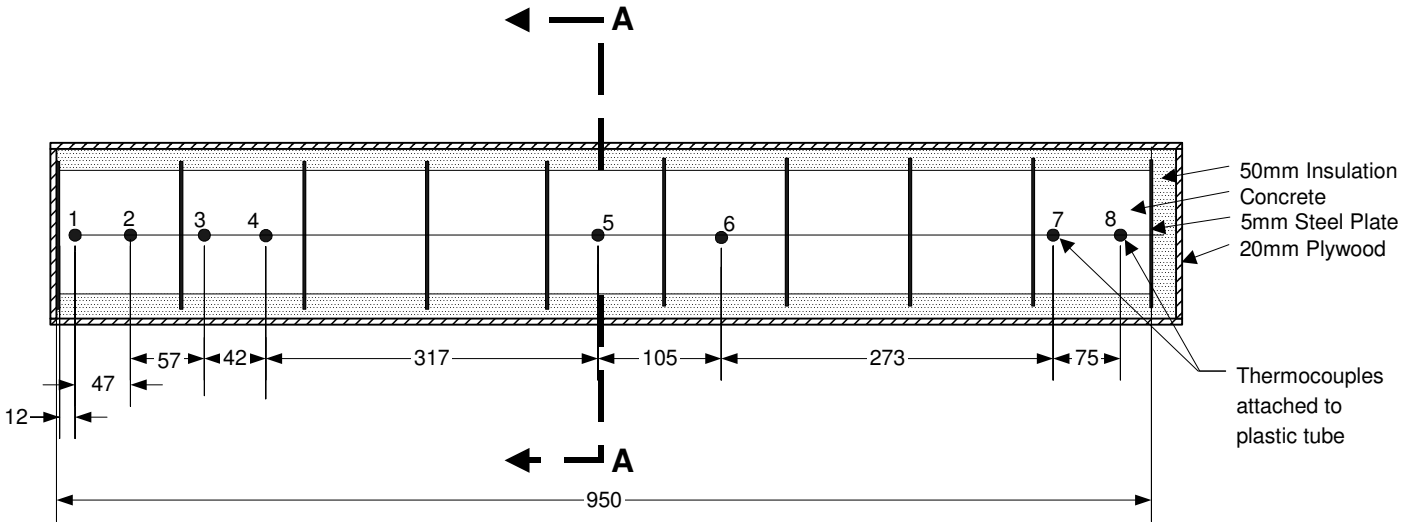

Fig. 2 Long Prism Details

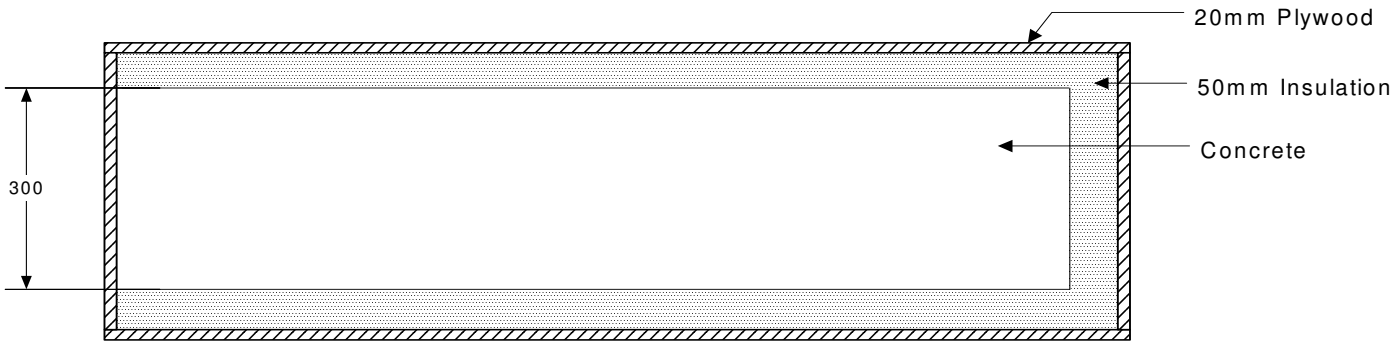

Sectional Elevation

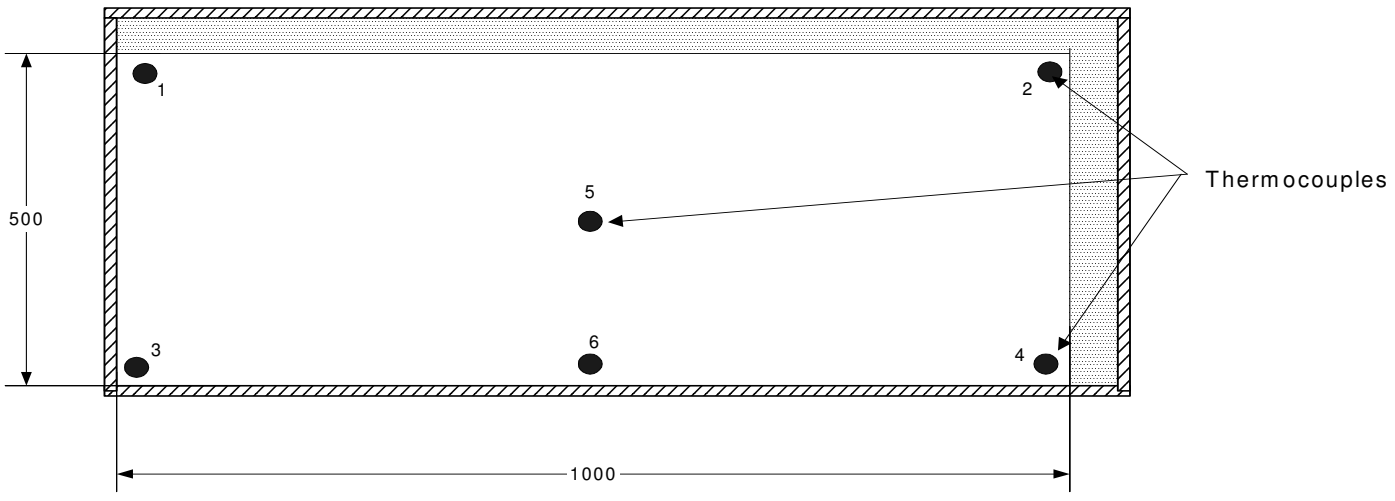

Sectional Plan

Fig. 3 Block Details

Fig. 4 Prism Number 2 (prior to pour)

Fig. 5 Block with temperature gauges (prior to pour)

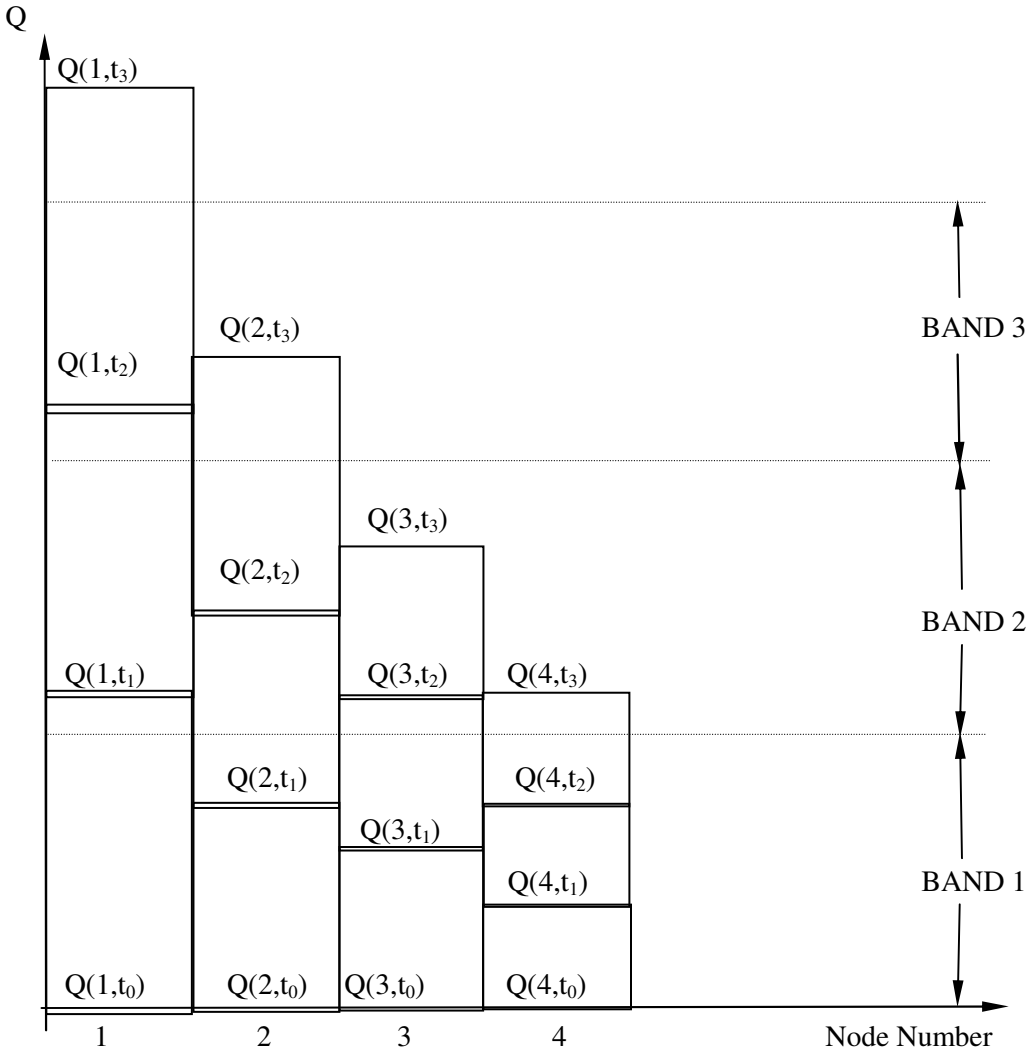

Fig. 6 Example of maturity bands for nodes along prism

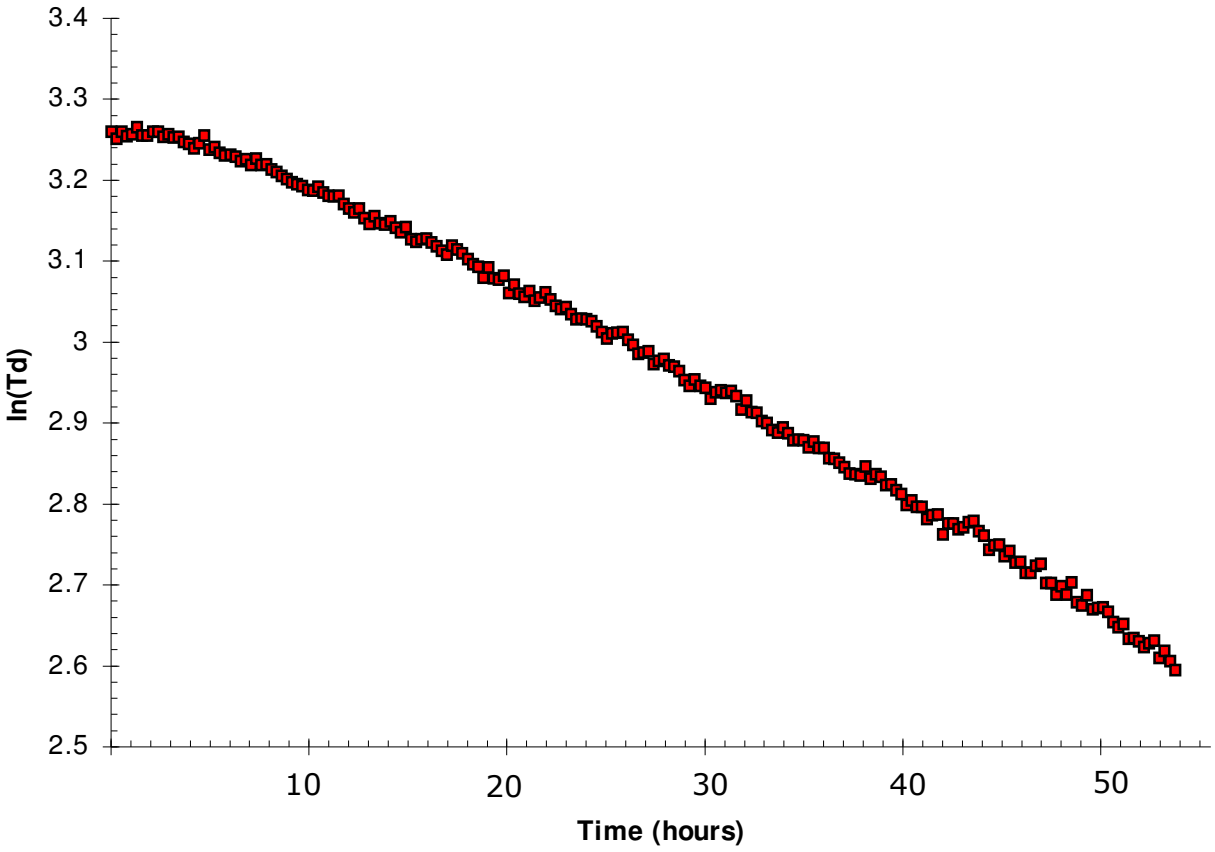

Fig. 7 Plot of log of T_d versus time for centre of long prism when losing heat

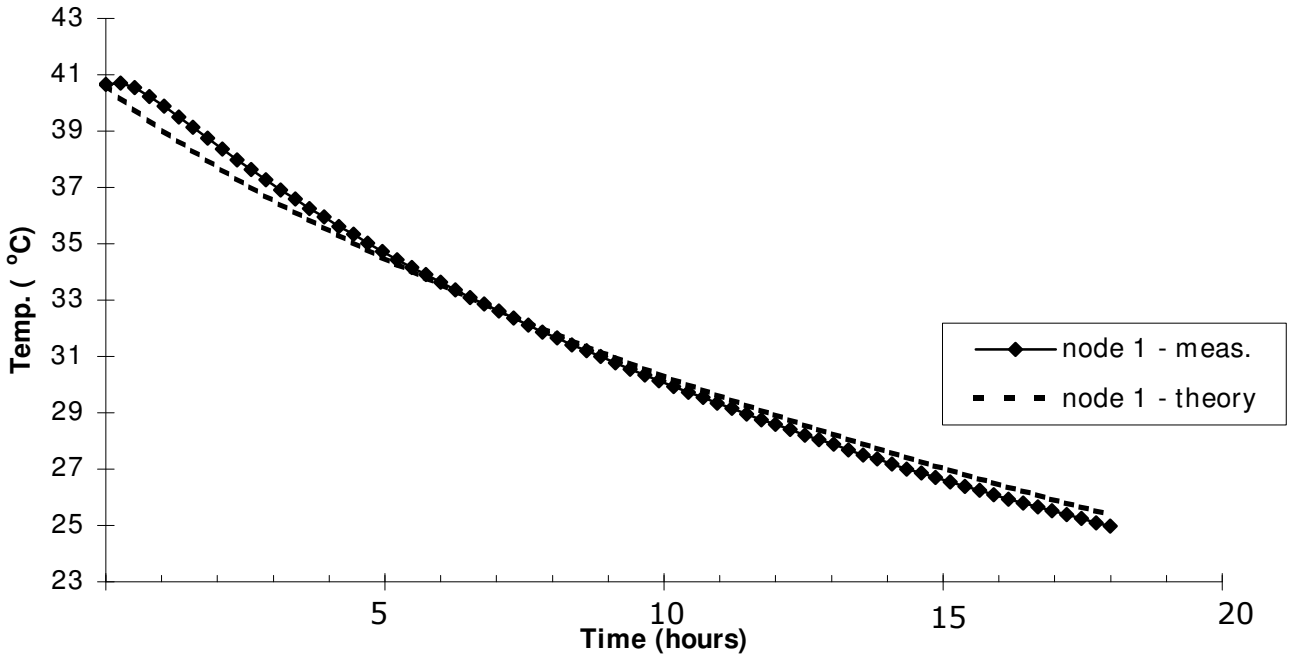

Fig. 8 Temperature versus time profile at Node 1 for long prism losing heat

Note: In all subsequent figures measured temperatures are shown as individual black squares and calculated temperatures as a solid line.

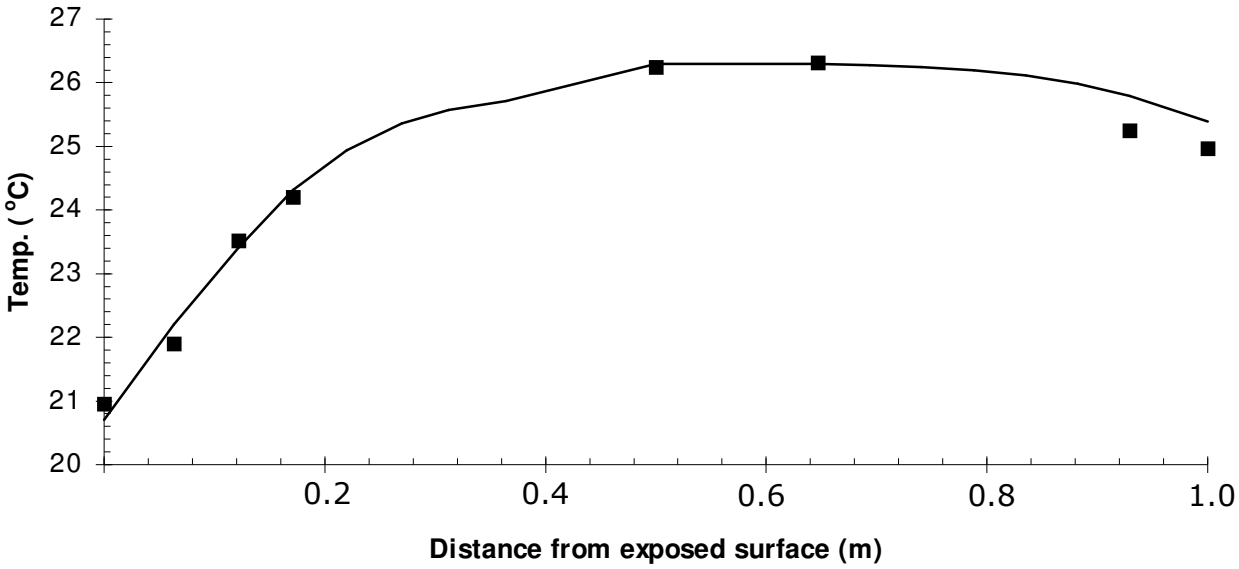

(a) Prism losing heat

Fig. 9 Temperature profile along the long prism axis at 22.75 hours

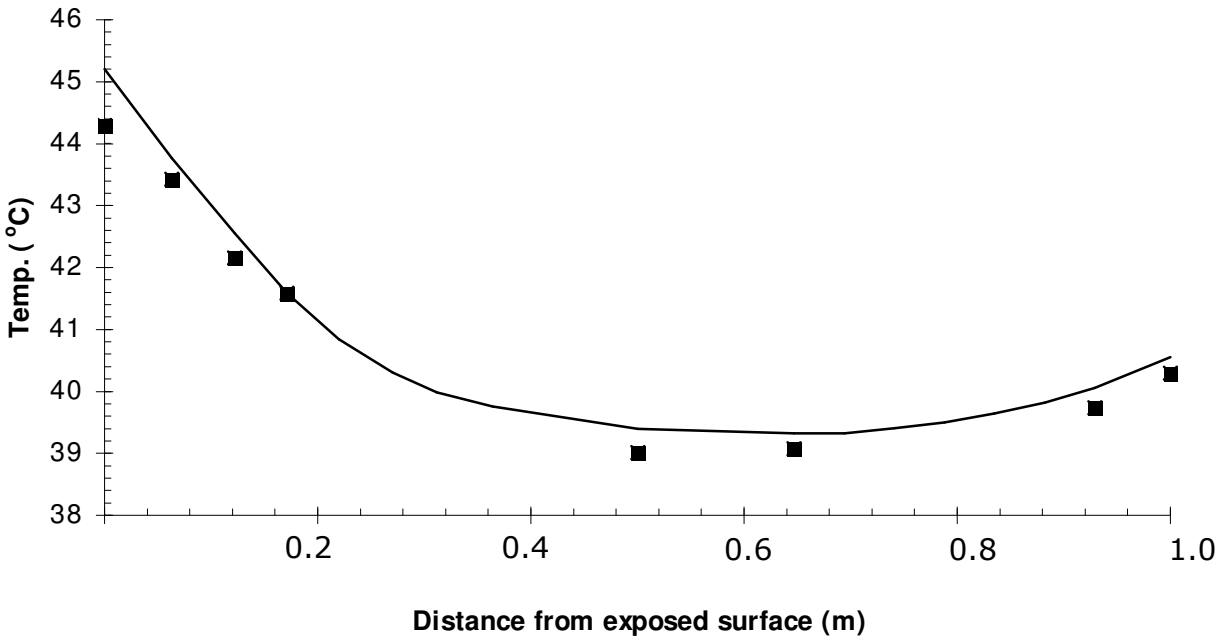

(b) Prism gaining heat

Fig. 9 Temperature profile along the long prism axis at 22.75 hours

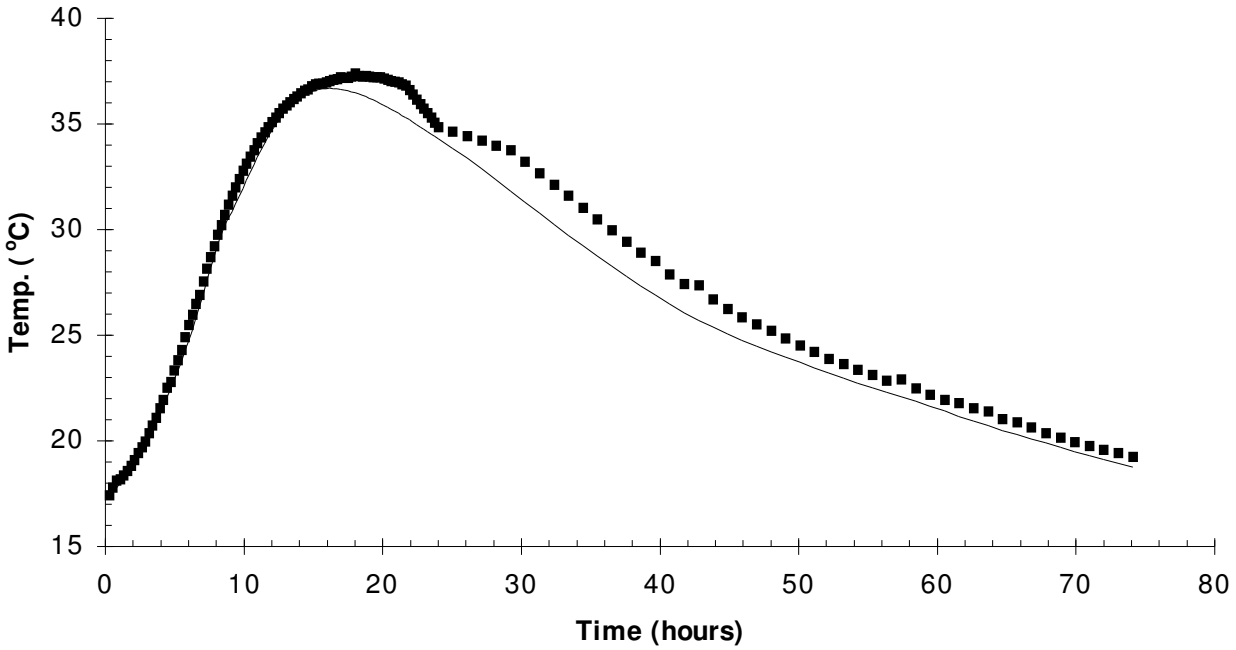

(a) Prism No. 1, Node 3

Fig. 10 Temperature Profiles in Short Prisms

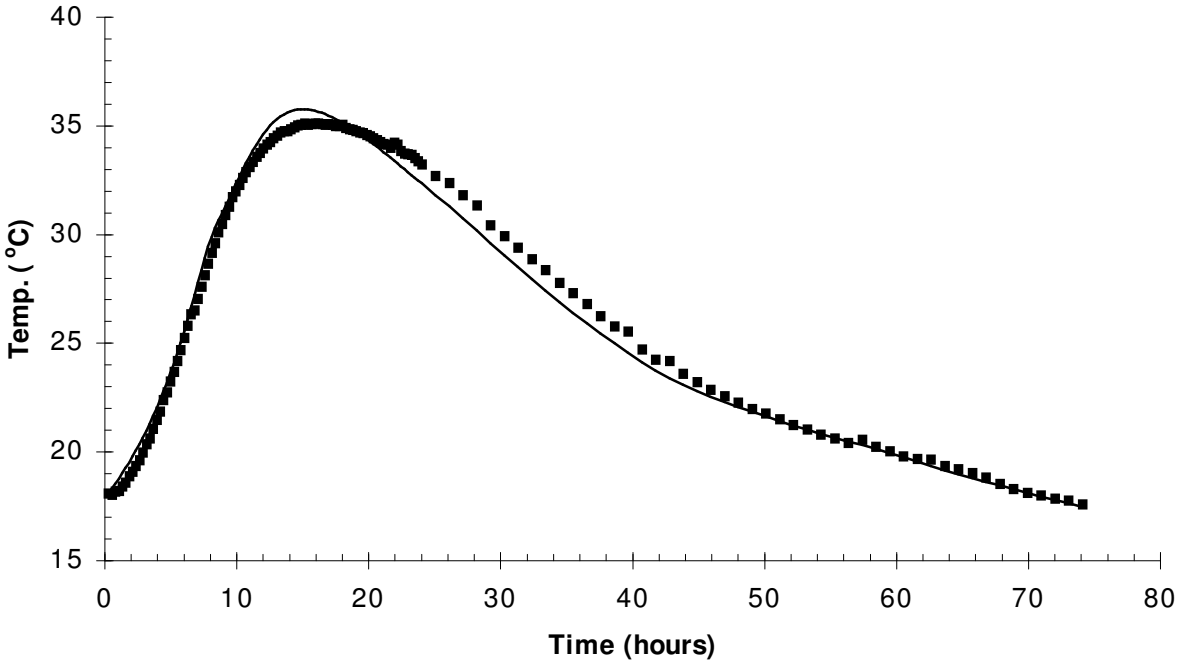

(b) Prism No. 3, Node 3

Fig. 10 Temperature Profiles in Short Prisms

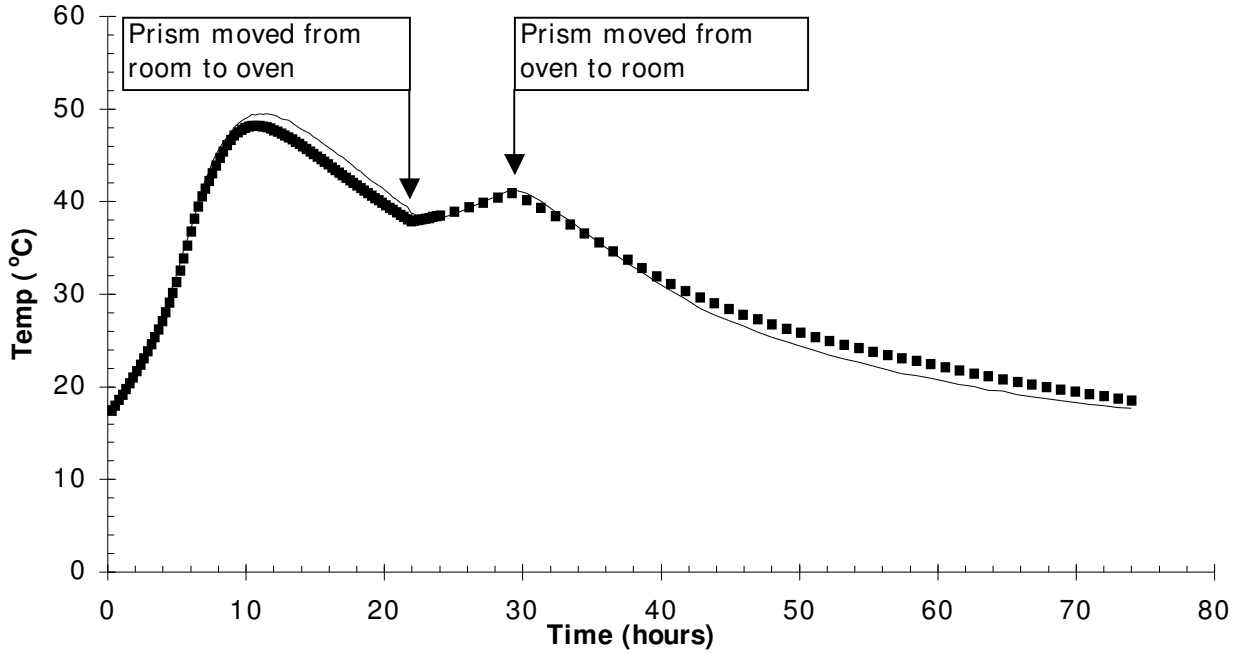

(c) Prism No. 2, Node 3

Fig. 10 Temperature Profiles in Short Prisms

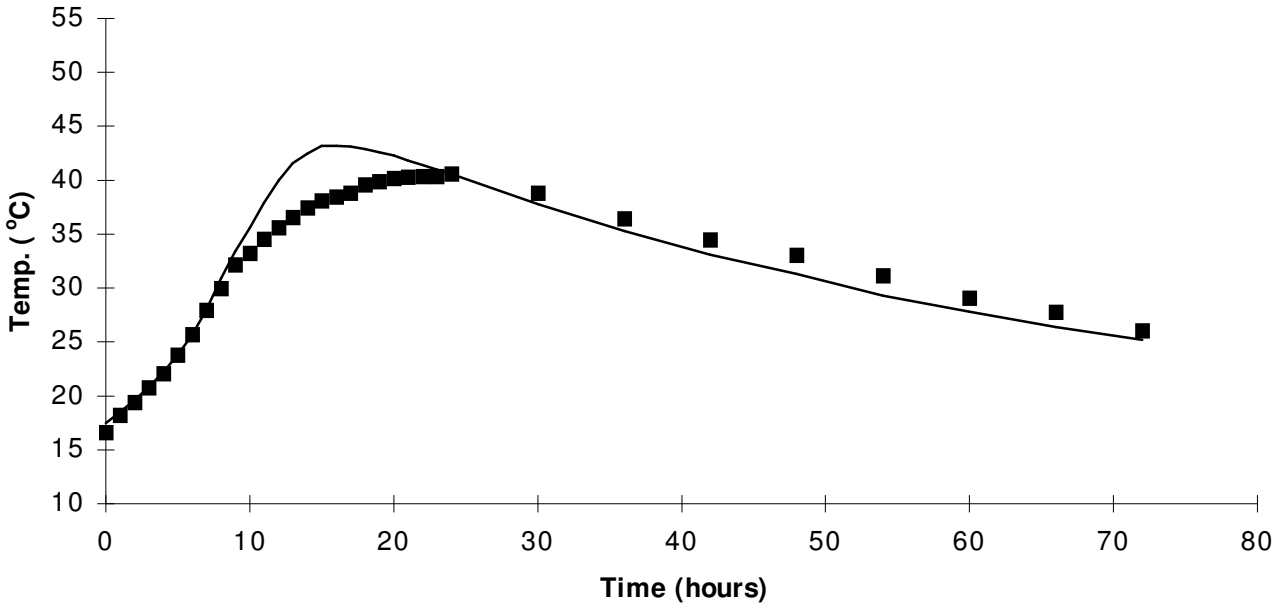

(a) Node 1

Fig. 11 Temperature versus time profiles in the Block

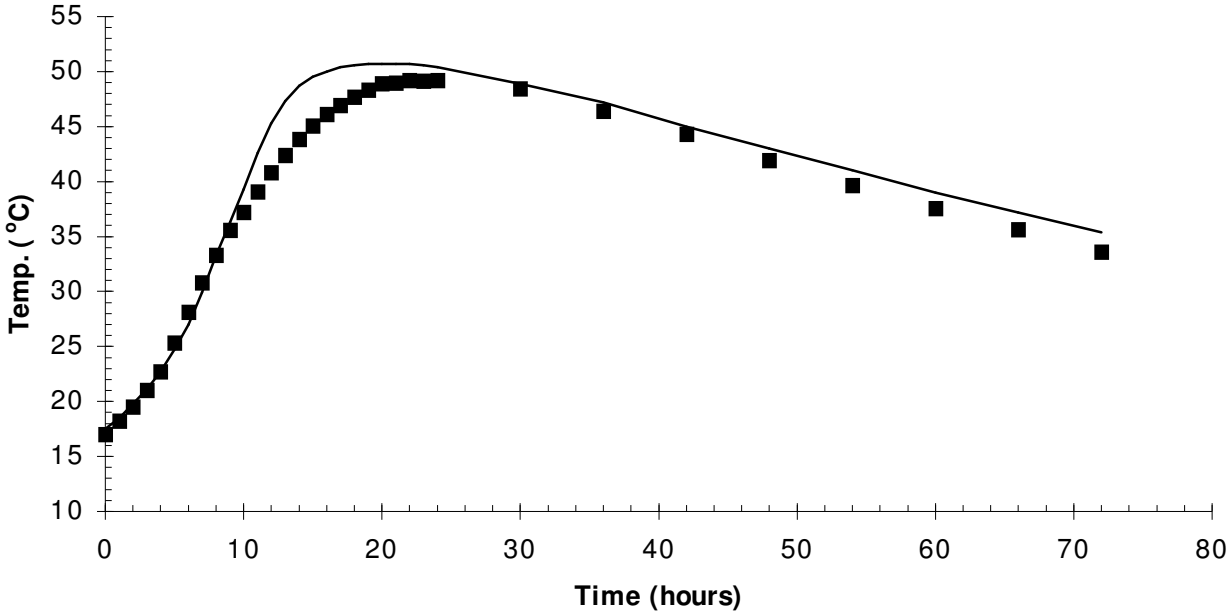

(b) Node 2

Fig. 11 Temperature versus time profiles in the Block

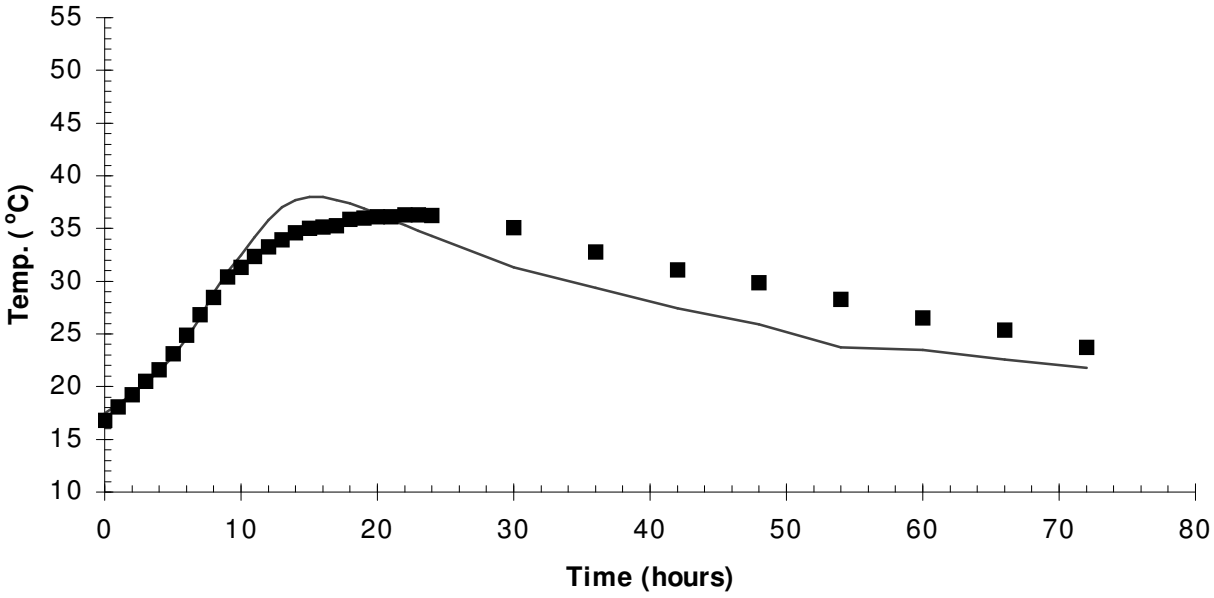

(c) Node 3

Fig. 11 Temperature versus time profiles in the Block

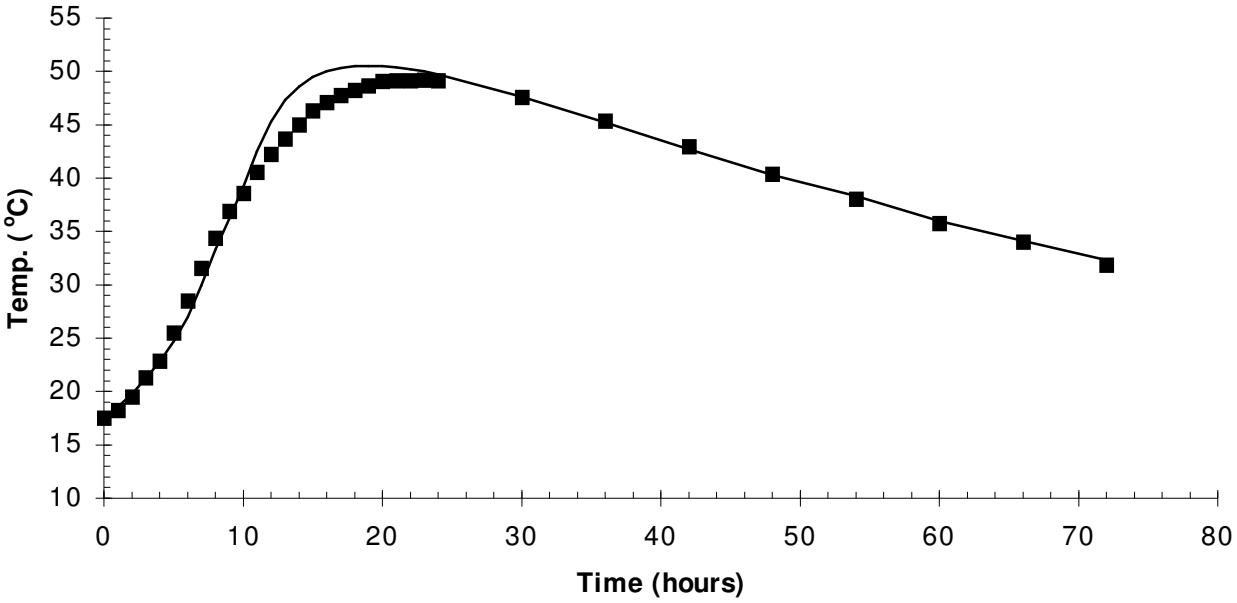

(d) Node 5

Fig. 11 Temperature versus time profiles in the Block

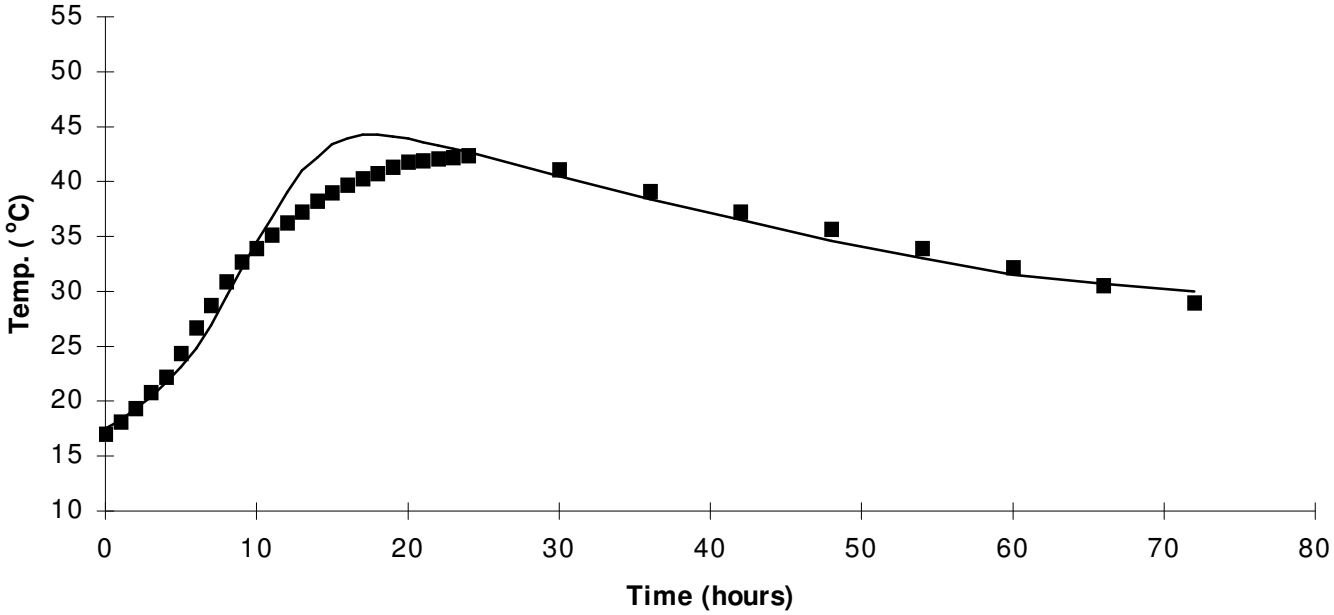

(e) Node 6

Fig. 11 Temperature versus time profiles in the Block

REFERENCES

1. Neville, A.M., (1995) *Properties of concrete* (4th Edition), Longman.

2. De Sitter, W.R. and Ramler J.P.G., (1991) "The Concrete Hardening Control System: CHCS" in *Testing during Concrete Construction*, *Proc. of an Int. RILEM Workshop,* ed. H.W. Reinhardt, Chapman & Hall, pp 224-243.

3. Harada, S., Suzuki, Y. and Maekawa, K., (1990) "Coupling analysis of heat generation and diffusion for massive concrete" in *Computer Aided Analysis and Design of Concrete Structures, Proceedings of SCI-C, Second International Conference*, ed. N. Bicanic, and H. Mang, Zel am See, Austria, pp.785-797.

4. Trinhztfy, H. W., Blauwendraad, J. and Jongendijk, J., (1981) "Temperature development in concrete structures taking account of state dependent properties", *International Conference on Concrete at Early Ages*, RILEM, pp 211-218.

5. Harrison, T. A., (1978) "Early age temperature rises in Concrete Sections with reference to B.S.5337:1976", *Interim Technical Note No. 5*, Cement & Concrete Association.

6. O'Brien, E.J., O'Donnell, J.J., Waldron, P. and El-H.Lahlouh., (1992) "Non-linear Conduction Modelling of Concrete Walls under the Influence of Heat of Hydration of Cement" in *Advanced Computational Methods in Heat Transfer II ,Vol. 1:Conduction,Radiation and Phase Change*, eds. R.C. Wrobel, C.A. Brebbia, A.J. Novak, Computational Mechanics Publications & Elsevier Applied Science,Milan, pp 121-130.

7. O'Donnell, J.J., O'Brien, E.J., Waldron, P. and El-H. Lahlouh., (1993) "Prediction of Early Age Strength in Concrete" in *Concrete 2000, Economic and durable construction through excellence, Vol. 1: Design,Materials,Construction*, eds. R.K. Dhir and M.R. Jones,E & FN Spon,Dundee, pp 839-845.

8. Rao, S.S., (1984) *Optimisation Theory and Applications*, John Wiley & Sons.

9. O'Brien, E.J. and O'Donnell, J.J., (1993) "The Effectiveness of Optimization Techniques for Material Property Characterization", in *Computational Methods and Experimental Measurements, Vol. 2: Stress Analysis*, eds. C.A. Brebbia and G.M. Carlomango, Computational Mechanics Publications & Elsevier Applied Science,Siena, pp 45-56.

10. Thurston, S. J., Priestley, M.J.N. and Cooke N., (1980) "Thermal Analysis of Thick Concrete Sections", *Journal of the American Concrete Institute*, 77, 5, Sept-Oct. 1980, pp 347-357.

11. Wang, C. and Dilger, W.H. (1995) "Prediction of Temperature Distribution in Hardening Concrete" in *Thermal Cracking in Concrete at Early Ages, Proc. of the Int. RILEM Symposium,* ed. R Springenschmid, E & FN Spon, pp 21-28.